

Radio Trends: Optically Identifying 20cm Sources (Data Provided)



Radio and Visual Images of the Crab Nebula, a Supernova Remnant

Submitted by:

Dennis Ward

HET-615

24 November, 2001

Project Advisor:

Pamela Gay

Abstract

In this paper, I determine the 20 brightest 20 cm radio sources within 30 degrees of the north galactic pole and within 10 degrees of the galactic plane, as found in the NRAO VLA Sky Survey (NVSS). After defining my sample population, I downloaded the corresponding images from the NVSS web site. These images were compared with optical images obtained from the Second Palomar Observatory Sky Survey (POSS II). By comparing the radio and optical images, I determined the optical counterpart of each radio source, thereby determining the radio source type (QSO, AGN, etc.). Since the sampling routine included sources from both within and outside our galaxy, it resulted in a varied population of source types, the distribution of which is analyzed herein.

Key words: surveys: NVSS — surveys: POSS II — galaxies: radio supernova remnants — radio sources

Introduction

Importance of 20 cm radio sources

The most abundant element in the universe is Hydrogen. It is a major component of the interstellar medium (ISM), as well as the primary component of stellar composition. When neutral atomic Hydrogen (HI) undergoes a spin-flip transition, it emits radio waves with a frequency of 1428 MHz (1.43 GHz), corresponding to a wavelength of 21 cm (Kaufmann & Freeman, 1998).

This 21 cm emission line is quite useful. Within our own galaxy, the intensity of the 21 cm line is a direct measure of the amount of HI present. Since this HI primarily is found within the ISM, mapping its concentration in our galaxy allows us to determine and begin to understand the structure of the Milky Way. However, nearly all the discrete radio sources located more than a few degrees from the Galactic plane are extragalactic. More than 99% of so-called “stronger” sources (>60 mJy at 1.4 GHz) are classical radio galaxies and quasars powered by supermassive black holes. Many of the fainter sources can be identified as low-luminosity AGN and star-forming galaxies containing ionized HII (Condon et al., 1998).

Importance of optical counterpart identification

As useful as 20 cm radio sources are for studying HI concentrations, radio galaxies, and the like, these radio observations alone can be hard to interpret. Consider the radio image contour in Figure 1. What is it—a radio jet from an active galactic nucleus (AGN), a supernova remnant (SNR), HI in the ISM, or something else?

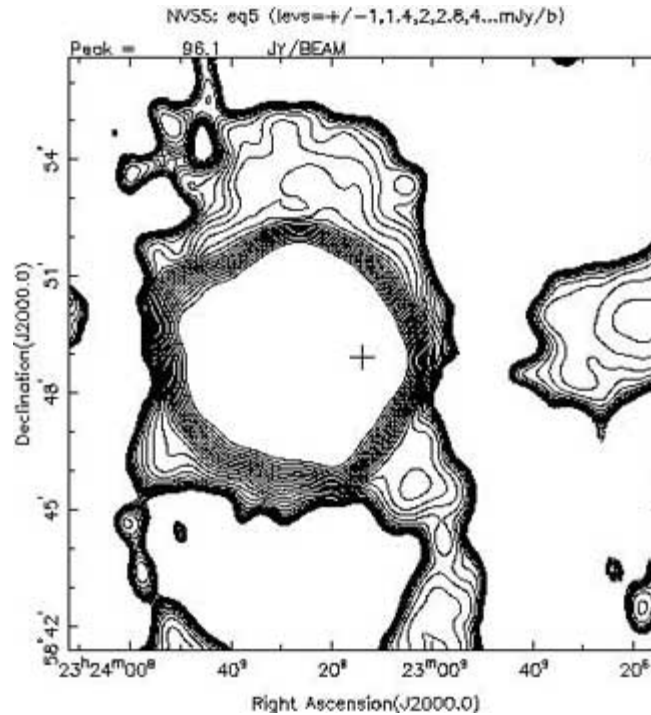


Figure 1. What is it?

In order to determine the origin of these radio sources, it is useful to identify the source's optical counterpart. Simply put, optical identification is the process of observing the same portion of the sky at optical wavelengths.

How is this identification accomplished? One might suppose that radio telescopes could be collocated with optical instruments that would provide an optical "snapshot" of each radio target. Fortunately, this is not necessary.

There have been a number of optical sky surveys performed in the past century. One of the most notable ones was the first Palomar Observatory Sky Survey (POSS I), conducted from 1949-57. POSS I covered the entire northern sky at red and blue wavelengths down to a declination of -33° (Reid et al., 1991).¹ This survey, along with its successor, the second Palomar Observatory Sky Survey (POSS II), is freely available from the Space Telescope Science Institute's (STScI) Digital Sky Survey (DSS) web page.²

These resources allow radio astronomers to more easily determine the source of a given radio emission. Using optical images from the POSS II survey, I will identify the optical counterparts of the 20 strongest radio sources around the North galactic pole (NGP) and the 20 strongest sources within 10° of the galactic equator, according to the NRAO VLA Sky Survey (NVSS).

¹ This coverage was later extended to -45° at red wavelengths only.

² <http://archive.stsci.edu/dss/index.html>

Why NVSS and POSS II were chosen

The NVSS investigated more than 82% of the celestial sphere, mapping the entire sky north of -40° (J2000) at 20 cm (1.4 GHz). It was designed to detect thousands of the nearest AGN (Condon et al., 1998). Since it sampled the continuum emission with a bandwidth of ± 42 MHz, it also covered the 21 cm line at 1428 MHz—thereby mapping the HI in our own galaxy as well as the extragalactic sources. This extensive coverage of the sky at 1.4 GHz made NVSS the logical source of bright radio sources to investigate.

The Second Palomar Observatory Sky Survey (POSS II) duplicates the sky coverage of POSS I, but in three passbands: blue, red and near-infrared. POSS II also improves on POSS I in terms of limiting magnitude. POSS II has limiting magnitudes of $B_j = 22.5$ mag, $R_c = 20.8$ mag, and $I_c = 19.5$ mag (Reid et al., 1991). The photographic plate emulsions have also improved dramatically since the 1950s. The DSS archive of POSS II plates currently provides coverage of 95% of the sky visible from Palomar in the red wavelengths and 50% in the blue wavelengths, using plates exposed from 1984-2000. Containing 95% of the northern sky imaged down to 20.8 mag, the DSS POSS II archive was chosen as the source of optical images. Additionally, the fact that the VLA in New Mexico and Palomar in California are at almost the same latitude (approximately 36° and 33° , respectively) ensures that their sky coverages are complimentary.

Data Collection & Reduction

Mining the NVSS Catalogue

The first step in compiling my target list of radio sources was to calculate the J2000 equatorial coordinates of the North galactic pole (NGP) as well as the range of coordinates needed to span the galactic equator.

Determining the target field coordinates for the sources near the NGP was straightforward. The J2000 coordinates for the NGP are $\alpha=12^\circ 51.42'$ and $\delta=27^\circ 07.8'$ (Leinert et al., 1998).

Determining the equatorial coordinates that correspond to the galactic equator required an algorithm to convert galactic longitude and latitude to R.A and declination. Fortunately, the *NED Coordinate Calculator* handles these conversions.³ Using the online calculator, the J2000 coordinates for every ten degrees of galactic longitude around the galactic equator were determined. A table containing the derived coordinates is found in Appendix A.

Armed with these J2000 coordinates, the NVSS Source Catalog Browser was used to generate two lists of bright radio sources.⁴ This web page allows the user to enter an equatorial coordinate, along with a search radius and a desired minimum peak flux density in mJy. When the search page is submitted, it returns an ASCII-formatted list of coordinates and flux density values, along with other values irrelevant to this project.

³ <http://nedwww.ipac.caltech.edu/forms/calculator.html>

⁴ <http://www.cv.nrao.edu/NVSS/>

To generate the desired polar population, the 20 brightest sources within 30° of the NGP, the following values were input:

Equinox:	J2000
Minimum Peak Flux Density:	2000 mJy
Central Right Ascension:	12 51 25.2
Central Declination:	27 07 48
Search Radius:	108,000 arcsec

The search engine returned 28 entries that matched these parameters. This list was then imported into Excel and sorted by flux density. The 20 brightest sources were then selected to comprise the polar population. Appendix B contains the polar population target list.

The equatorial population target list was generated in the same manner, except that the minimum flux density was set to 5000 mJy and the search radius was reduced to 54,000 arcsec. The 36 sets of coordinates representing the galactic equator were input five at a time, using the “batch mode” provided by the NVSS Source Catalog Browser. The sources thus returned were imported into Excel for further manipulations.

Since the equatorial coordinates entered were spaced 10° apart and the search radius was set to 15° , there was a fair amount of overlap, which of course caused duplicate entries to be retrieved. This overlap was necessary to prevent a vignetting effect due to the circular search pattern used. Sorting the list by flux density and inspecting all duplicate densities to make sure their coordinates were also duplicates eliminated these duplicate entries.

The galactic equator is inclined to the celestial equator so that its declination ranges from approximately $+63^\circ$ to -63° . The NVSS however, only covers the sky down to -40° in declination. This means that about 85 degrees of the galactic equator, corresponding to a galactic longitude of $\sim 260^\circ$ – 345° , will not be included in the target population sample.

The remaining entries were then filtered to remove those that were more than 10° away from the galactic equator. This left approximately 40 sources that were then reduced to the 20 brightest. The equatorial population thus obtained is contained in Appendix C.

Gathering the NVSS data

Once the two target lists were created, it was time to start gathering the radio data from the NVSS. Another online resource, the NVSS Postage Stamp Server,⁵ was used to obtain NVSS data in two formats, FITS images and PostScript contour plots.⁵

For each of the 40 target fields, a FITS image file, containing a $.25 \times .25$ degree area around the target's centroid coordinates was downloaded. The pixel spacing and size was set to 2 arcseconds per pixel, making the image scale similar to that of the POSS II

⁵ <http://www.cv.nrao.edu/NVSS/postage.html>

images described below. In addition, a contour plot formatted as a PostScript file was also generated and retrieved using the same settings as the FITS image.

While reviewing the NVSS data returned by the server, it was discovered that one of the target fields, EQ18, was not well formed. After reviewing both the FITS data and the contour plot, I determined that this field fell on the edge of one of the few remaining holes in the NVSS data. A quick search of the NVSS web site confirmed that there was in fact a small gap in coverage in this area. In order to have 20 fields to study, the 21st strongest source in the equatorial listing was added as EQ21.

Gathering the POSS II images

Since the digitized version of the POSS II survey is 95% complete in the red wavelengths, as opposed to only 50% in blue, the red plate images were downloaded for each target list entry. The STScI-DSS online form was used to obtain .25x.25 degree FITS images for each target centroid.⁶ These images match the fields-of-view of the NVSS data previously obtained.

Reducing the data

Unfortunately, the DSS retrieval tool does not allow the user to adjust the pixel spacing and size. Although the NVSS FITS images were obtained using setting to most closely match the scale of the POSS II images, this scaling was not exact. In order to produce comparison images with identical scales, the MIRA AP application was used to resample the NVSS images to match the POSS II images. MIRA AP was also used to create 3D surface plots of representative radio source types as shown in Figures 3 & 4, as well Appendices D & E.

Likewise, the NVSS contour plots did not match the now-standard image scale, and needed to be resampled. There were two added complications regarding the contour plots. First, they were formatted as PostScript files, which MIRA AP cannot read. Second, in addition to the actual contour plot, these images contained additional information, such as text labels and coordinate grids, as shown in Figure 1.

In order to make the contour plots easier to compare to the POSS II images, it was necessary to first convert the PostScript files to bitmapped GIF files. The GIF images were then cropped so that only the actual contour plot remained, and then resized to match the POSS II images. These conversions and manipulations were accomplished using the GhostView and Photoshop programs.

At this point, a library of 120 identically scaled images was ready for identification and analysis.

⁶ <http://stdu.stsci.edu/dss/>

Analysis and Discussion

Target identification

The process of target identification consisted of three phases:

1. Visual identification of optical target types
2. Identification based on SIMBAD search results
3. Reconciling the visual and SIMBAD results

In order to make an initial visual identification of the 40 target fields, they were loaded into MIRA AP for viewing. They were centered and crosshairs were placed automatically at the target coordinate centroid. After examining each target field, a type determination was made based on the observed morphology. This initial analysis resulted in the following distribution:

	<u>Polar</u>	<u>Equatorial</u>
Stars	13	4
Galaxies	4	0
SNRs	0	11
Nebulae	0	2
Empty/Unknown	<u>3</u>	<u>3</u>
Total	20	20

In the second phase, both target lists were submitted as appropriately formatted ASCII files to the SIMBAD server.⁷ SIMBAD returned the following classifications:

	<u>Polar</u>	<u>Equatorial</u>
QSOs	11	3
Galaxies	9	1
SNRs	0	13
Nebulae	0	0
Empty/Unknown	<u>0</u>	<u>3</u>
Total	20	20

In order to reconcile the differences between the visual and SIMBAD identifications, it was necessary to carefully review each image, comparing them to the SIMBAD search results. The final reconciled classifications are summarized here:

	<u>Polar</u>	<u>Equatorial</u>
QSOs	9	2
Galaxies	8	1
SNRs	0	12
Nebulae	0	2
Empty/Unknown	<u>3</u>	<u>3</u>
Total	20	20

While it would have been tempting to simply accept the SIMBAD classifications, that was not feasible, since the purpose of this project was to identify optical counterparts to

⁷ <http://simbad.harvard.edu/sim-flist.pl>

each of the NVSS radio sources. In the cases where there were no identifiable objects in the POSS II fields, it was necessary to record those as empty fields, rather than the faint objects reported by SIMBAD. Conversely, many of the POSS II images showed the sources as stellar images, while SIMBAD reported them as quasars (QSOs). In these cases, I went with the SIMBAD classification.

The final target identifications may be found in Appendix D.

Target types (QSOs, SNRs, etc.)

As previously shown, the optical counterparts for the 40 targets can be broken down into five basic target types: quasars, galaxies, supernova remnants, nebulae, and empty fields.

Quasars (QSOs) are extragalactic objects that have very small angular sizes and high redshifts. Approximately 10% of all known quasars are strong radio emitters. Their spectra contain stellar-type absorption lines, consistent with the idea that quasars are embedded within remote galaxies. Most astronomers are convinced that a quasar is an extremely brilliant active galactic nucleus, powered by a supermassive black hole, so remote and highly luminous compared with the galaxy within which it is embedded that, in most cases, only the compact nucleus can be seen (Encyclopedia of Astronomy and Astrophysics, 2000b). Quasars are such strong radio emitters that they easily outshine all other objects within the combined sample except the radio galaxy M87, which also contains a supermassive black hole, and account for 11 (27.5%) of the 40 target fields.

Some galaxies, known as radio galaxies, can have radio luminosities up to a million times that evidenced by a normal galaxy (Encyclopedia of Astronomy and Astrophysics, 2000c). Like quasars, these galaxies are thought to derive their radio brightness from the accretion discs surrounding supermassive black holes. Nine radio galaxies make up 22.5% of the target list.

Supernova remnants (SNRs) are the aftermath of a stellar explosion, including interstellar gas swept up in a shock wave, the expanding stellar debris and in some cases a compact stellar remnant. Some SNRs are powered by pulsars, while others show no sign of a neutron star or black hole (Encyclopedia of Astronomy and Astrophysics, 2000d). Twelve SNRs are found in the target list, representing 30% of the target population.

Emission nebulae account for just 5% of the target list (2 out of 40). Most shine because the gas from which they are composed is ionized by ultraviolet radiation from a nearby star; examples are H II regions and planetary nebulae (Encyclopedia of Astronomy and Astrophysics, 2000a). The observed 1.43 GHz emissions are indicative of HI in the ISM associated with the nebulae.

The final 15% of the target list are the six empty fields. There are two main explanations for why there are no optical counterparts for these fields. The first is that the optical counterpart could be too faint to be imaged by the POSS II plates. The second is that the optical counterpart could be offset from the observed radio feature, as in the case of a radio jet streaming from a faint galaxy.

Radio source power distribution & morphology

In addition to identifying the optical counterparts for each of the radio sources, the two populations were also analyzed to determine their power distribution and morphology.

Figure 2 plots the total flux for each radio source in mJy against a logarithmic scale. The equatorial population sources evidence flux that is almost ten times that seen in the polar population.

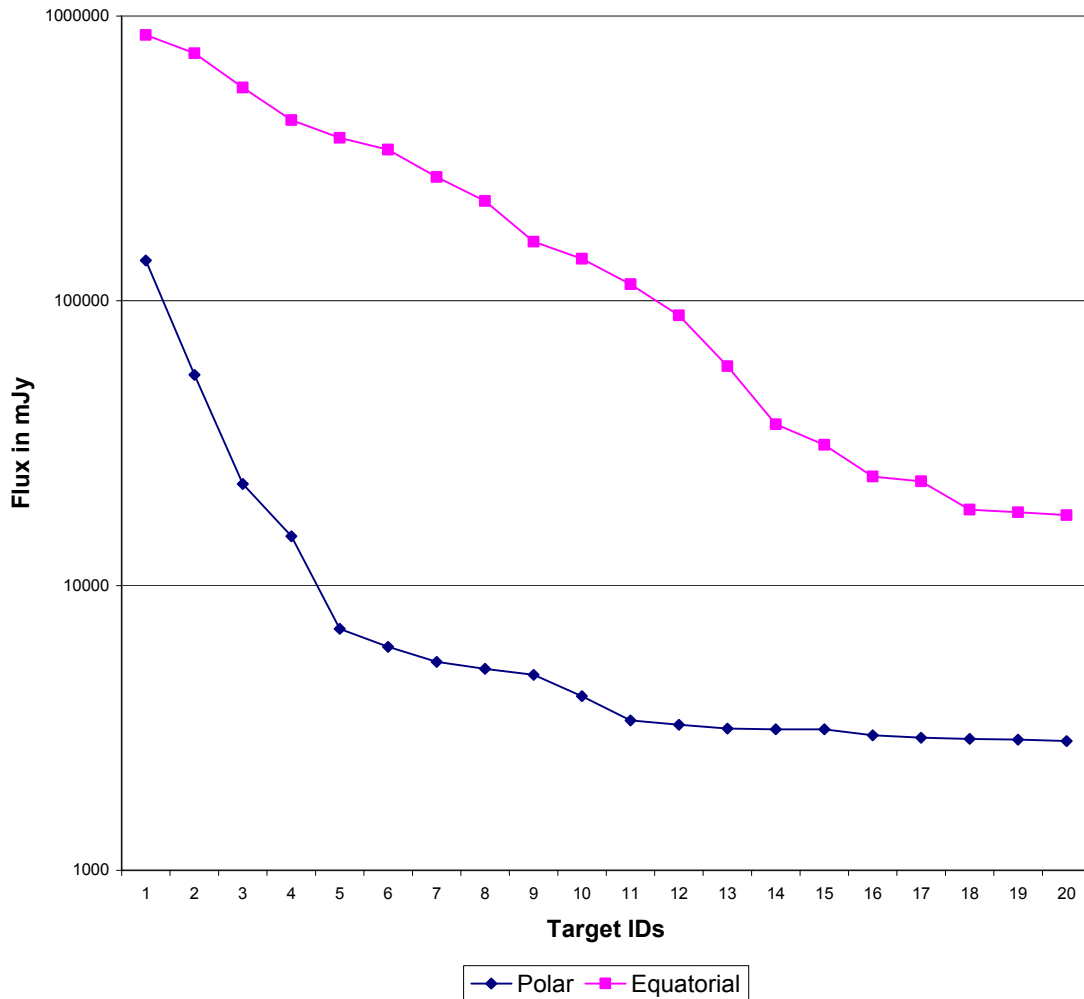


Figure 2. Power Distribution of Radio Sources

The morphology of the 40 radio sources fell into two categories: point sources as represented by Figure 3, and extended sources as shown in Figure 4. Optically, the point sources are made up of quasars and radio galaxies, for the most part. The extended sources correspond to SNRs and nebulae.

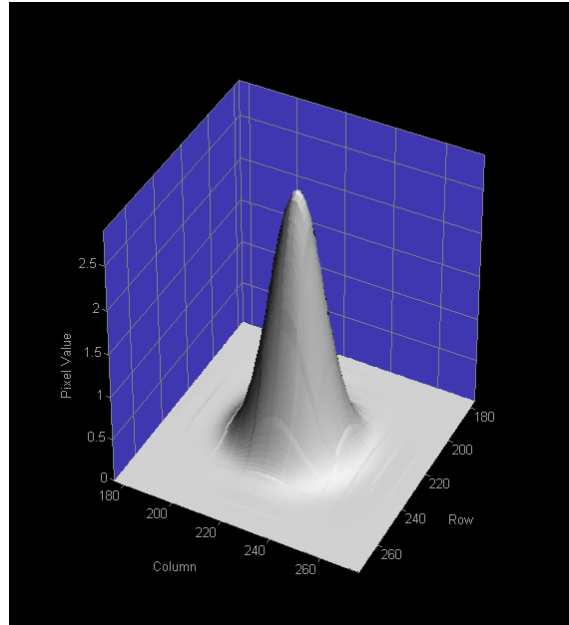


Figure 3. Radio Point Source (QSO 1153+3144)

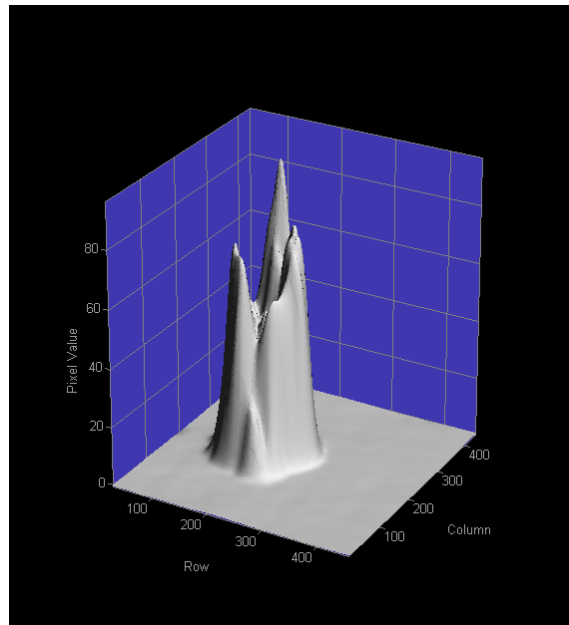


Figure 4. Extended Radio Source (CAS A)

A detailed breakdown of the distribution of point vs. extended sources is provided in the next section.

Comparing polar and equatorial populations

The primary reason for splitting up the target list into polar and equatorial populations was so that a comparison could be made as to the differential makeup of the two

populations. In other words, what type of sources are visible in each population and why?

To review, the polar population is made up of the 20 brightest radio sources within 30° of the north galactic pole (NGP), while the equatorial population is comprised of the 20 brightest sources within 10° of the galactic equator.

What differences would be expected between the two populations? The most obvious difference is that the equatorial population is directly in the plane of the galaxy, and as such, should contain mostly those objects that exist within our galaxy. The polar population, on the other hand, should be made up primarily of extragalactic objects, since they are located 90° from the galactic plane.

In fact, this is precisely what was observed.

	<u>Polar</u>	<u>Equatorial</u>
QSOs	9	2
Galaxies	8	1
SNRs	0	12
Nebulae	0	2
Empty/Unknown	3	3
Total	20	20

The polar population is made up entirely of extragalactic objects—9 quasars and 8 galaxies. According to the SIMBAD database, the three empty fields are also extragalactic objects, 2 QSOs and a galaxy, too faint to register on the POSS II plates.

Approximately 70% of the equatorial population is made up of objects found inside our galaxy. SNRs and nebulae must be within our galaxy in order to show up on the POSS II plates. The other 30% of this population is made up of quasars, empty fields, and a radio galaxy. This too makes sense. The quasars are so bright that they outshine all other radio sources found in the plane of the galaxy, placing them at the top of the list when sorted by flux density. The lone galaxy in the equatorial list, M94, outshines all but the 13 sources stronger than it in the galactic plane. While SIMBAD identifies one of the three remaining empty fields as a QSO, the other two could either be extragalactic sources or perhaps faint SNRs located within our galaxy.

Problems associated with matching optical and radio images

One of the problems that must be addressed when identifying optical counterparts is the positional accuracy of the various catalogs and data used. Typically, optical astrometry yields positional data that is far more accurate than positions given by radio observations alone. The NVSS positions reported at 1.4 GHz have rms uncertainties of approximately 1 arcsecond in right ascension and declination (Condon et al., 1998). The POSS II positions are accurate to approximately 0.15 arcseconds (Anonymous, 2001; Reid et al., 1991). Extreme care was taken to ensure that the radio and visual images were properly registered.

One of the more puzzling aspects of the identification of optical counterparts for the equatorial population was that numerous radio sources corresponded to the same optical target. For example, equatorial targets 3-6 and 13 are all contained within the SNR known as Cassiopeia A. Targets EQ 7, 8, and 10-13 are all found within the M1, the Crab Nebula. Even the two brightest targets, EQ 1 & 2, were both associated with a quasar known as QSO 1957+405. Upon reflection, these multiple identifications make sense, as they occurred in extended objects, whose intensities vary on a scale discernable by the VLA as configured for the NVSS.

The final problem is best represented by the six fields that produced no optical counterparts. In these cases, the red POSS II plates did not record an object at that bandpass down to approximately magnitude 20.8. In these cases, the counterparts were either too faint to register or did not emit light at those wavelengths.

Conclusion

In this paper, I determined the 20 brightest 20 cm radio sources within 30 degrees of the north galactic pole and within 10 degrees of the galactic plane, as found in the NRAO VLA Sky Survey (NVSS). After defining my sample population, I downloaded the corresponding images from the NVSS and compared them with optical images obtained from the Second Palomar Observatory Sky Survey (POSS II).

By comparing the radio and optical images, I determined the optical counterpart of each radio source, thereby determining the radio source type (QSO, AGN, etc.). Since my sampling routine included sources from both within and outside our galaxy, it resulted in a varied population of source types, the distribution of which was analyzed.

As expected, the polar population consisted exclusively of extragalactic targets, while the equatorial population consisted of a mix of galactic and extragalactic targets.

References

- Anonymous. (2001). *Digitized Sky Survey*, [Web site]. STScI. Available: <http://stdatu.stsci.edu/dss/> [2001, 17 September].
- Condon, J. J., Cotton, W. D., Greisen, E. W., Yin, Q. F., Perley, R. A., Taylor, G. B., & Broderick, J. J. (1998). The NRAO VLA Sky Survey. *Astronomical Journal*, *115*, 1693-1716.
- Cotton, W. D. (1999a, 4 May). *NVSS Postage Stamp Server*, [Web site]. NRAO. Available: <http://www.cv.nrao.edu/NVSS/postage.html> [2001, 10 September].
- Cotton, W. D. (1999b, 21 January). *NVSS Source Search*, [Web site]. NRAO. Available: <http://www.cv.nrao.edu/NVSS/> [2001, 10 September].
- Encyclopedia of Astronomy and Astrophysics. (2000a). Nebula. In P. Murdin (Ed.), *Encyclopedia of Astronomy and Astrophysics*. Bristol: Institute of Physics Publishing.
- Encyclopedia of Astronomy and Astrophysics. (2000b). Quasar. In P. Murdin (Ed.), *Encyclopedia of Astronomy and Astrophysics*. Bristol: Institute of Physics Publishing.
- Encyclopedia of Astronomy and Astrophysics. (2000c). Radio Galaxy. In P. Murdin (Ed.), *Encyclopedia of Astronomy and Astrophysics*. Bristol: Institute of Physics Publishing.
- Encyclopedia of Astronomy and Astrophysics. (2000d). Supernova Remnants. In P. Murdin (Ed.), *Encyclopedia of Astronomy and Astrophysics*. Bristol: Institute of Physics Publishing.
- Kaufmann, W. J., & Freeman, R. A. (1998). *Universe* (5th ed.). New York: W. H. Freeman and Company.
- Leinert, C., Bowyer, S., Haikala, L. K., Hanner, M. S., Hauser, M. G., Lèvasseur-Regourd, A.-C., Mann, I., Mattila, K., Reach, W. T., Schlosser, W., Staude, H. J., Toller, G. N., Weiland, J. L., Weinberg, J. L., & Witt, A. N. (1998). The 1997 reference of diffuse night sky brightness. *Astronomy and Astrophysics Supplement Series*, *127*, 1-99.
- Reid, I. N., Brewer, C., Brucato, R. J., McKinley, W. R., Maury, A., Mendenhall, D., Mould, J. R., Mueller, J., Neugebauer, G., Phinney, J., Sargent, W. L. W., Schombert, J., & Thicksten, R. (1991). The second Palomar Sky Survey. *Publications of the Astronomical Society of the Pacific*, *103*, 661-674.

Appendix A

J2000 Coordinates for the Galactic Equator

Gal Latitude	Gal Longitude	RA	DEC
0	0	17h45m37.21597s	-28d56m10.1847s
0	10	18h07m45.72953s	-20d17m24.0352s
0	20	18h27m31.78945s	-11d29m18.9003s
0	30	18h46m05.22954s	-02d36m32.9069s
0	40	19h04m22.93044s	+06d17m13.7512s
0	50	19h23m19.02084s	+15d08m32.5088s
0	60	19h43m54.35875s	+23d53m25.2218s
0	70	20h07m27.92337s	+32d26m32.7171s
0	80	20h35m53.13578s	+40d39m48.7968s
0	90	21h12m01.09512s	+48d19m46.3921s
0	100	22h00m00.89074s	+55d02m59.1377s
0	110	23h04m31.54516s	+60d09m34.0893s
0	120	00h25m48.21227s	+62d43m31.9775s
0	130	01h52m17.14204s	+62d02m01.2367s
0	140	03h07m15.15354s	+58d17m51.2886s
0	150	04h04m28.06062s	+52d25m12.3930s
0	160	04h46m58.42308s	+45d14m46.2813s
0	170	05h19m29.45099s	+37d18m53.9346s
0	180	05h45m37.17006s	+28d56m10.1911s
0	190	06h07m45.67418s	+20d17m24.1644s
0	200	06h27m31.73215s	+11d29m19.0624s
0	210	06h46m05.18614s	+02d36m32.9485s
0	220	07h04m22.89857s	-06d17m13.6772s
0	230	07h23m18.99825s	-15d08m32.3310s
0	240	07h43m54.32265s	-23d53m25.2341s
0	250	08h07m27.87973s	-32d26m32.7326s
0	260	08h35m53.10078s	-40d39m48.9418s
0	270	09h12m01.04710s	-48d19m46.7542s
0	280	10h00m00.82879s	-55d02m59.6356s
0	290	11h04m31.47331s	-60d09m34.7300s
0	300	12h25m48.15074s	-62d43m32.6403s
0	310	13h52m17.12291s	-62d02m01.8307s
0	320	15h07m15.17795s	-58d17m51.7944s
0	330	16h04m28.10725s	-52d25m12.7700s
0	340	16h46m58.48629s	-45d14m46.5140s
0	350	17h19m29.50921s	-37d18m53.9746s
0	360	17h45m37.21597s	-28d56m10.1847s

Appendix B

The Polar Population Target List

	RA (2000)			DEC			Flux	Gal
	h	m	s	d	m	s	mJy	Lat
1	12	30	49.46	12	23	21.6	138487.0	74.49
2	12	29	06.41	02	03	05.1	54991.2	64.36
3	14	11	20.63	52	12	09.0	22720.1	60.80
4	13	31	08.31	30	30	32.4	14902.7	80.67
5	13	30	37.69	25	09	11.0	7052.2	80.98
6	14	19	08.18	06	28	36.3	6100.3	60.66
7	13	47	33.42	12	17	24.1	5397.2	70.17
8	12	56	57.38	47	20	19.8	5099.6	69.76
9	13	26	16.51	31	54	09.7	4861.9	81.05
10	13	52	17.81	31	26	46.7	4085.4	76.06
11	13	38	49.67	38	51	11.1	3358.9	74.66
12	14	23	00.81	19	35	22.8	3247.0	67.71
13	14	21	05.73	41	44	49.7	3146.9	66.56
14	11	43	25.04	22	06	56.0	3128.7	73.77
15	11	14	38.43	40	37	20.8	3127.9	65.93
16	11	56	18.74	31	28	05.0	2978.3	77.24
17	12	54	11.68	27	37	32.7	2923.9	89.21
18	12	43	57.63	16	22	52.7	2895.8	79.11
19	10	58	58.69	43	01	23.7	2875.1	62.25
20	12	20	33.88	33	43	10.9	2845.9	80.64

Appendix C

The Equatorial Population Target List

	RA (2000)			DEC			Flux	Gal
	h	m	s	d	m	s	mJy	Lat
1	19	59	32.07	40	43	47.9	858423.0	5.74
2	19	59	24.03	40	44	19.2	739766.0	5.77
3	23	23	25.58	58	50	21.4	560780.0	-2.11
4	23	23	26.27	58	47	38.2	431380.0	-2.15
5	23	23	13.84	58	48	54.9	373100.0	-2.12
6	23	23	39.44	58	48	34.2	339504.0	-2.14
7	05	34	32.28	22	00	31.1	272168.0	-5.78
8	05	34	35.30	22	00	34.3	224272.0	-5.77
9	17	45	42.24	-29	00	15.8	161188.0	-0.06
10	05	34	25.46	22	01	59.3	140549.0	-5.79
11	05	34	28.83	22	00	19.3	114404.0	-5.80
12	05	34	31.80	22	02	13.8	88971.4	-5.77
13	05	34	40.23	21	59	49.0	58893.0	-5.76
14	19	23	42.51	14	30	31.1	36825.1	-0.39
15	19	10	15.43	09	06	19.1	31205.5	0.00
16	23	23	37.17	58	50	07.8	24161.9	-2.12
17	17	24	45.08	-34	10	32.4	23227.3	0.90
18	18	20	26.89	-16	12	23.5	18806.8	-0.70
19	06	27	10.06	-05	53	06.1	18486.1	-8.06
20	17	18	01.20	-37	26	33.8	18092.3	0.16
21	02	25	44.10	62	06	07.8	17674.7	1.22*

* Target No. 21 was added to compensate for a problem with No. 18, as discussed in the text.

Appendix D

Final Target Identification List

The Polar Population:

	Flux (mJy)	Type	Identification
P1	138487.0	galaxy	M87
P2	54991.2	QSO	3C 273C
P3	22720.1	QSO	QSO 1409+524
P4	14902.7	galaxy	3C 286 G1
P5	7052.2	QSO	J133037.7+250911
P6	6100.3	QSO	J141908.2+062835
P7	5397.2	QSO	QSO 1345+125
P8	5099.6	EF	Empty Field
P9	4861.9	galaxy	4C 32.44
P10	4085.4	galaxy	UCG 8782
P11	3358.9	galaxy	3C 288
P12	3247.0	EF	Empty Field
P13	3146.9	galaxy	3C 299
P14	3128.7	EF	Empty Field
P15	3127.9	galaxy	J111438.6+403720
P16	2978.3	QSO	QSO 1153+3144
P17	2923.9	galaxy	3C 277.3
P18	2895.8	QSO	J124357.7+162253
P19	2875.1	QSO	QSO 1056+432
P20	2845.9	QSO	J122033.9+334312

The Equatorial Population:

	Flux (mJy)	Type	Identification
EQ1	858423.0	QSO	QSO 1957+405
EQ2	739766.0	QSO	QSO 1957+405
EQ3	560780.0	SNR	Cassiopeia A
EQ4	431380.0	SNR	Cassiopeia A
EQ5	373100.0	SNR	Cassiopeia A
EQ6	339504.0	SNR	Cassiopeia A
EQ7	272168.0	SNR	Crab Nebula
EQ8	224272.0	SNR	Crab Nebula
EQ9	161188.0	EF	Empty Field
EQ10	104549.0	SNR	Crab Nebula
EQ11	114404.0	SNR	Crab Nebula
EQ12	88971.4	SNR	Crab Nebula
EQ13	58892.0	SNR	Crab Nebula
EQ14	36825.1	GAL	M94
EQ15	31205.5	EF	Empty Field
EQ16	24161.9	SNR	Cassiopeia A
EQ17	23277.3	nebula	NGC 6357
EQ18	18806.8	(removed)	
EQ19	18486.1	EF	Empty Field
EQ20	18092.3	SNR	SNR 349.7+00.2
EQ21	17674.7	nebula	IC 1805

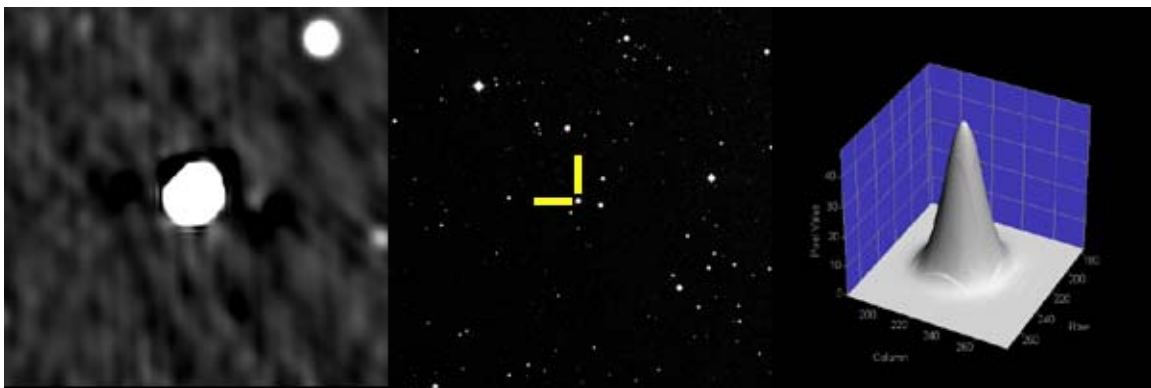
Appendix D

Sample Images—Polar Population

Each of the following images is made up of three views of the same target field. From left to right they are the NVSS radio image, the POSS II visual image, and a 3-D plot of the NVSS image.



Target P1, Radio Galaxy M87



Target P2, Quasar 3C 273C

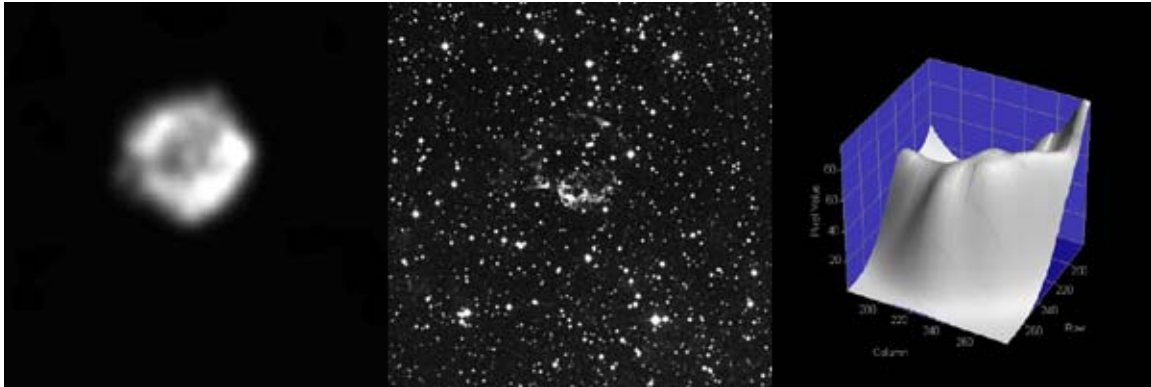


Target P10, Radio Galaxy UCG 8782
(Note the radio “lobes” oriented 90° from the plane of the galaxy.)

Appendix E

Sample Images—Equatorial Population

Each of the following images is made up of three views of the same target field. From left to right they are the NVSS radio image, the POSS II visual image, and a 3-D plot of the NVSS image.



Target EQ3, Supernova Remnant Cassiopeia A



Target EQ8, Supernova Remnant Crab Nebula



Target EQ17, Emission Nebula NGC 6357